

Theoretical analysis of linear optical properties of PbS_xSe_{1-x} (X=0.5)

التحليل النظري للخواص البصرية الخطية للمركب PbS_xSe_{1-x}(x=0.5)

Mazin S. Othman¹

Department of General Science, Faculty of Education, Soran University, Soran-Erbil,
Iraq, mazin.othman@soran.edu.iq
TeL: +964(0) 750 4809690

Samir M. Hamad²

Department of Mathematic, Faculty of Science, Soran University, Soran-Erbil, Iraq,
samir.hamad@soran.edu.iq
TeL.; +964(0) 7510685459

Hewa Y. Abdullah³

Department of Physics, College of Education Salahaddin University-Hawler
kuhewa@yahoo.com
TeL.; +964(0) 7504674832

Abstract

The optical properties of $x = 0.5$ value for of PbS_xSe_{1-x} ternary semiconductor alloys are calculated from the real and imaginary part of the dielectric function by using pseudopotential density functional method within its local density approximation (LDA) and a scissors approximation. A direct band gap of 0.49 eV at Γ is obtained for PbS_{0.5}Se_{0.5}. The starting value of absorption for PbS_xSe_{1-x} alloy of $x = 0.5$ semiconductor alloy is 0.49 eV. The energy loss function maximum has value 15.6A eV. Our results are in agreement with the available theoretical data in the literatures.

الخلاصة:

الخواص البصرية لقيمة (X=0.5) لسبائك اشباه موصلات ثلاثية PbS_xSe_{1-x} قد تم حسابها من الجزء الحقيقي والجزء الخيالي لدالة العزل باستخدام طريقة (Pseudo Potential Density Functional) باستخدام تقريب الكثافة الموضعية (LDA) وتقريب (Scissor). تم الحصول على فجوة الطاقة المباشرة بقيمة (0.49eV) في موقع الطاقة (Γ) للمركب PbS_{0.5}Se_{0.5}. بداية قيمة الامتصاص للسبيكة شبه الموصل PbS_xSe_{1-x} لقيمة (x=0.5) وكانت (0.49eV). القيمة العظمى لدالة فقد الطاقة كانت (15.6AeV). كانت نتائجنا متوافقة مع البيانات النظرية المتوفرة في الادبيات.

1. Introduction

IV–VI compound semiconductors have shown remarkable potential for a various applications and commercial technologies, ranging from conventional transistor based electronics to optoelectronics devices. Therefore, IV–VI semiconductors have been widely used for high-electron mobility and heterostructure bipolar transistors, lasers diode (LD), light emitting diodes (LED), photodetectors, electro optic modulators, and frequency-mixing components [1–4].

In addition, group IV–VI semiconductors and their heterostructures are well-known to form ternary and quaternary alloys with a direct band gap over most of alloy composition range with high absorption coefficients, which can be used as materials for fabricating thin film heterojunction photovoltaic (PV) devices. The two compounds PbS and PbSe, which are direct band gap semiconductors at the Γ point of the Brillouin zone, form a continuous series of alloys denoted by PbS_{1-x}Se_x, where x is the mole fraction of PbSe in the alloy. This alloys system has received

considerable attention for the fabrication of tunable diode lasers. The energy band gap of $\text{PbS}_{1-x}\text{Se}_x$ alloys varies from 0.29 eV for PbS to 0.15 eV for PbSe. [5, 6]

Experimental researches have been performed on their structural and optical properties [7-10]. Despite of experimental studies, there are also many theoretical studies are describing the electronic structures of these compound semiconductors by using different methods of calculations. Lebedev and Sluchinskaya have found the appearance of ferroelectricity in these IV-VI semiconductors, and they investigated the samples of $\text{PbS}_x\text{Se}_y\text{Te}_{1-x-y}$ quaternary solid solutions at low temperatures by using electrical and x-ray methods [11]. Also, Seetawan *et al.* have reported the simulation mechanical properties of PbS, PbSe [12]. Wang *et al.*, have investigated the plane-wave pseudopotential of mechanical and electronic properties for IV and III-V crystalline phases with zinc-blende structure [13]. The vacuum evaporated $\text{PbS}_{1-x}\text{Se}_x$ thin films were examined by Kumar *et al.*, [14], on the other hand, multi-spectral of $\text{PbS}_x\text{Se}_{1-x}$ photovoltaic infrared detectors were realized by Schoolar *et al* [15].

This work has been done to shed light on the future studies of scientists whose experimentally prepare the alloys in laboratories, and to support them in determining the change in amounts of additives in alloy, moreover, to determine the accordance of theoretical studies with experiments and other theoretical works. The optical properties of $\text{PbS}_x\text{Se}_{1-x}$ will change x function ($x=0.5$) which directly influences various applications of PbS-based devices under different application conditions. Taking into account of different application conditions, the Structure and optical properties of alloy is studied by using first-principles calculations in our work.

2. Computational Method

The physical properties of $\text{PbS}_x\text{Se}_{1-x}$ alloys are investigated using the CASTEP program [16]. The model wurtzite is used in $\text{PbS}_x\text{Se}_{1-x}$ alloy. We apply a 16-atom super cell which corresponds to a $2 \times 2 \times 1$ that is twice the size of the primitive wurtzite unit cell in basic plane direction. In this program the calculation is performed using Kohn–Sham formation [17], which is based on the density function theory (DFT). Local density approximation (LDA) is made for electronic exchange correlation potential energy. Coulomb potential energy caused by electron–ion interaction is described using pseudo-potential concept. The optimized non-local pseudo-potential generated using the scheme proposed by Liuo *et al.* [18] and is adopted, in which tee orbitals of Pb (5d 6s 6p), S (3s 3p) and Se (3d 4s 4p) are treated as valence electrons. By the non-conserving condition, the pseudo wave function is related to pseudo-potential matches and the plane-wave function expanded with Kohn–Sham formation beyond cutoff energy.

A cubic unit cell is constructed with four Group VI atoms (Se/S). We have considered $\text{PbS}_x\text{Se}_{1-x}$ alloy as having cubic symmetry in our calculation for all the five systems to maintain consistency and simplicity. We expect that for $x = 0.5$ the alloy is a layered structure and should be non-cubic.

Geometry optimization is performed for $\text{PbS}_x\text{Se}_{1-x}$ with symmetry P1. Atomic positions are relaxed and optimized with a density mixing scheme [19] using the conjugate-gradient (CG) method [20] for eigenvalues minimization. The iteration is repeated until the energy is less

than 0.002 meV/atom. The Monkhorst- Pack scheme [21] with uniform mesh points is applied.

3. Results and discussion

The lattice constant of the compound are estimated In the first step of calculations, by minimizing the lattice parameters of the crystal structure, i.e. the ratio of total energy of the crystal to its volume. The tested optimization setup convergence is shown in Fig.1. Bulk module is also obtained for individual structure.

CASTEP Optimization Convergence

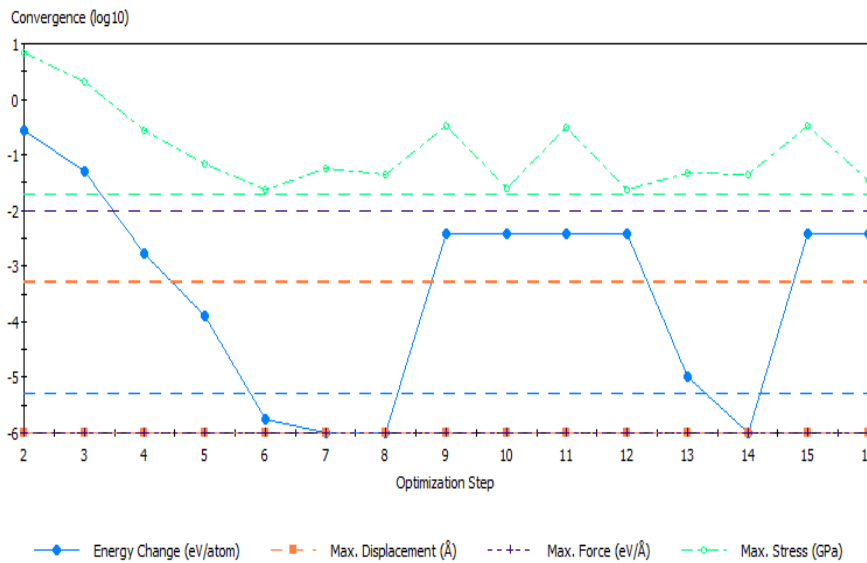


Figure 1. The optimization setup convergence of $x = 0.5$ value for PbS_xSe_{1-x} alloy.

From this calculation, the obtained values of the bulk module are found to be 1% less than the theoretical value. The results of lattice parameters for $x = 0.5$ are given in Table1. By using these lattice parameters, the electronic band structures corresponding to high symmetry points are calculated. Fermi level is adjusted as a zero energy level.

Table1; Calculated equilibrium lattice constants (a_0), bulk modulus (B) and results of other theoretical works of PbS_xSe_{1-x} alloy.

PbS_xSe_{1-x}	Reference	a_0 (Å)	E_g (eV)	B (GPa)
$x = 0.5$	Present	5.97	0.49	61.8
$x = 0.5$	Theory ^a	6.12	0.36	48.4
$x = 0.5$	Theory ^b	5.95	0.40	63.6
$x = 0.5$	Theory ^c	6.12	-----	53.6

^a Ref. [22].

^b Ref. [23].

^c Ref. [24].

From the drawn band structures, it is found that these structures have direct band rang symmetry point at the center of Brillouin zone. The optical band gap energy value is equal to 0.49 eV. This value is in agreement with theoretical values.

Semiconductors behave as absorbers for short wavelength photons and as transparent for long wavelength photons [25]. Absorption or transition of a photon depends on the photon's energy, prohibited energy range of semiconductor and the arrangement of atoms [26]. The optical coefficients, such as absorption coefficient, loss function and dielectric function are key issue for optoelectronic devices and their applications.

To investigate the optical properties of PbS_xSe_{1-x} ($x = 0.5$) alloy, it is important to study the imaginary part of the dielectric function $\epsilon_2(\omega)$. It is familiar that, the interaction between photon and electrons in the materials can be explained in terms of time dependent perturbations of the electronic ground state. Optical transitions between occupied and unoccupied states are caused by electric field of the photons. The momentum matrix elements are obtained between occupied and unoccupied states, in turns used to calculate the $\epsilon_2(\omega)$ function. Calculating these matrix elements, one uses the corresponding eigenfunctions of each of the occupied and unoccupied states.

Using the Density function theory (DFT), the excitability electronic spectrum of material is generally described according to the complex dielectric frequency function, $\epsilon(\omega) = \epsilon_1(\omega) + i\epsilon_2(\omega)$, both the real part and the imaginary part of complex dielectric function are containing all of the desired reaction information. The real and imaginary parts are related with the Kramers–Kronig correlations:

$$\epsilon_1(\omega) = 1 + \frac{2}{\pi} \int_0^{\infty} \frac{\epsilon_2(\omega') \omega' d\omega'}{\omega'^2 - \omega^2} \tag{1}$$

$$\epsilon_2(\omega) = \frac{Ve^2}{2\pi\hbar m^2 \omega^2} \int d^3k \sum_{mm'} |\langle kn | p | kn' \rangle|^2 f(kn) \times [1 - f(kn')] \delta(E_{kn} - E_{kn'} - \hbar\omega) \tag{2}$$

Since the optical properties of the solid material are reactions between electrons and the time dependent electromagnetic perturbation caused by the light absorption, the calculation of the optical properties of the solid means calculation of the optical reaction function, i.e. the complex dielectric function. Some optical constants can be obtained by using the dielectric function [27, 28]. Real components of the function can be calculated from imaginary components of dielectric function, energy loss function, refraction index (n) and attenuation coefficient (k) which are determined by the components of dielectric tensor;

$$L(\omega) = -\text{Im} \left(\frac{1}{\epsilon} \right) = \frac{\epsilon_2(\omega)}{[\epsilon_1^2(\omega) + \epsilon_2^2(\omega)]} \tag{3}$$

$$\alpha(\omega) = \sqrt{2\omega} [\sqrt{\epsilon_1^2(\omega) + \epsilon_2^2(\omega)} - \epsilon_1(\omega)]^{1/2} \tag{4}$$

Figure 2 shows the real and imaginary components of the linear dielectric function, for each structure, it is based on the photon energy of alloys calculated at cubic and tetragonal phases. By using these results of dielectric functions, the energy loss function coefficient $L(\omega)$ and absorption coefficient $\alpha(\omega)$ can be calculated.

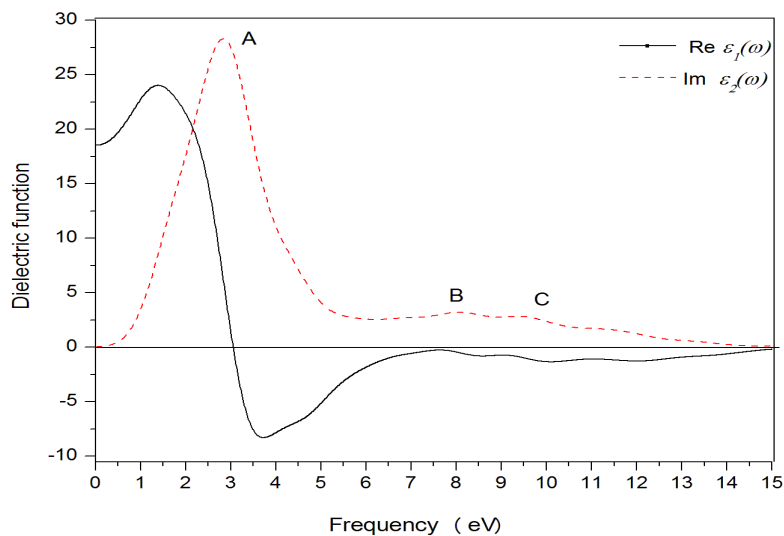


Figure 2. The real and imaginary parts of dielectric function.

the real and imaginary parts of dielectric function of PbS_xSe_{1-x} alloy $x = 0.5$ formed based on S add to PbSe structure, are given in comparison. As illustrated in Fig.2, the real part of the dielectric function increased with the increasing photon energy out of the region between 0.5 and 1.2 eV and this is a normal distribution. In contrast, it decreases as the photon energy increased in the region between 1.2 and 3.6 eV. This is an abnormal dispersion characteristic. A strong absorption and increase in reflection between 1.2 to 3.6 eV has been observed. This compound semiconductor has a fundamental absorption limit at infrared spectrum regions. The importance of these regions rises up especially for communication devices applications of such alloys [29]. This will be seen in more detail in the absorption and reflectivity curves to be given later on.

The peak values of imaginary parts of dielectric function based on photon energy as shown in Fig. 2 are present in Table 2. These peak values correspond to electronic transition from valence band to conduction band (optical transitions).

Table 2 characteristic of linear optical function PbS_xSe_{1-x}

PbS_xSe_{1-x}	A (eV)	B (eV)	C (eV)
$x = 0.5$	2.79	8.50	11.21

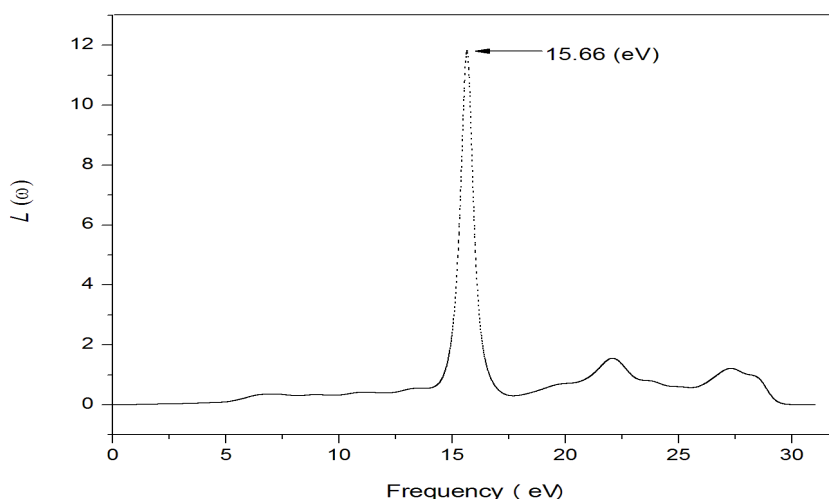


Figure 3. Loss of function of $x = 0.5$ of PbS_xSe_{1-x} alloy.

Energy loss function defines the energy loss of the electrons passing between bands; energy loss function of alloy according to x value is calculated by using Eq. (3). The definite of maximum energy loss function are related to collective vibrations of valence electrons. Subsequently, as shown in Fig. 3, the energy loss function maximum at $x = 0.5$ of PbS_xSe_{1-x} alloy is based on S add to PbSe structure has a value of 15.6 eV.

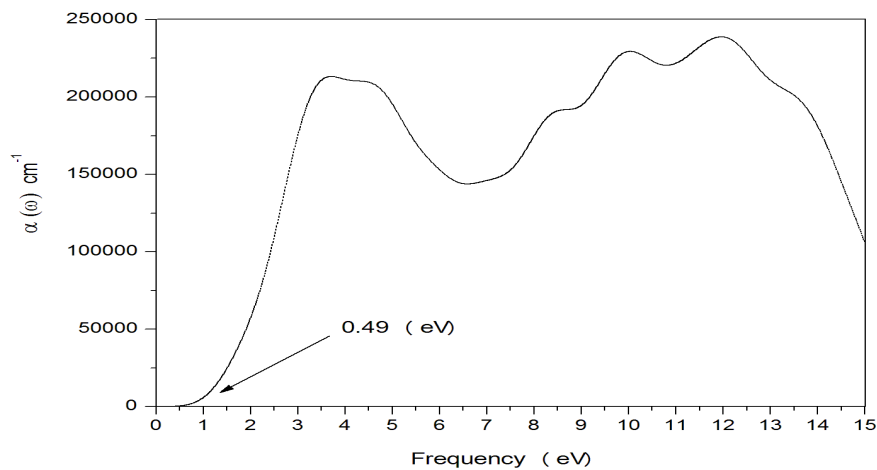


Figure 4. Optical absorption of $x = 0.5$ of $\text{PbS}_x\text{Se}_{1-x}$ alloy.

Figure 4, shows the optical absorption spectra of the $x = 0.5$ of $\text{PbS}_x\text{Se}_{1-x}$ alloy under the scissor operation. Due to the underestimation of the band gap, it is difficult to obtain the exact optical energy band gap. This method is operative for a variety of systems. The starting value of absorption point is 0.49 eV. It is well known that the relation between the optical band gap and the absorption coefficient is given by [29];

$$\alpha h\nu = c(h\nu - E_g)^{1/2}$$

Where h is the Planck constant, c is the constant for a direct transition, ν is the frequency of radiation, and α is the optical absorption coefficient. The optical band gap E_g can be obtained from the intercept of $(h\nu)^2$ versus photon energy $(h\nu)$.

4. Conclusion

The optical properties of the $\text{PbS}_x\text{Se}_{1-x}$ alloy of $x = 0.5$ have been studied by using the first-principles calculation based on the plane-wave pseudopotentials method within the LDA approximation. The lattice parameters, bulk modulus and energy band gap have been obtained. The optical band gap energy increased from 0.31 to 0.49 eV with increasing S concentration. These results are in agreement with other theoretical studies. The starting value of absorption for $\text{PbS}_x\text{Se}_{1-x}$ alloy of $x = 0.5$ semiconductor alloy is 0.49 eV. The considered optical properties are consistent with the available experimental results.

Acknowledgements

The authors would like to thanks Dr. Srwa Saeed and Assistant Researcher Murad Sherzad for their assistance in suggestions and discussions.

Reference

- [1] M. Othman, E. Kasap & N. Korozlu. (2010). Ab-initio investigation of structural, electronic and optical properties of $\text{In}_x\text{Ga}_{1-x}\text{As}$, $\text{GaAs}_{1-y}\text{P}_y$ ternary and $\text{In}_x\text{Ga}_{1-x}\text{As}_{1-y}\text{P}_y$ quaternary semiconductor alloys. *Journal of Alloys and Compounds*, 496 (1), 226–233.
- [2] H-S Kim, I. Ok, M. Zhang and F. Zhu. (2008). A study of metal-oxide-semiconductor capacitors on GaAs, $\text{In}_{0.53}\text{Ga}_{0.47}\text{As}$, InAs, and InSb substrates using a germanium interfacial passivation layer. *Appl. Phys. Lett.*, 93(2), 062111.
- [3] M. Passlack, N. Medendorp, R. Gregory, D. Braddock. (2003) Role of Ga_2O_3 template thickness and gadolinium mole fraction in $\text{Gd}_x\text{Ga}_{0.4-x}\text{O}_{0.6}/\text{Ga}_2\text{O}_3$ gate dielectric stacks on GaAs. *Appl. Phys. Lett.*, 83 (1) 5262.
- [4] Mazin SH. Othman. (2012). Structural and Optical Properties of $\text{GaAs}_{0.5}\text{Sb}_{0.5}$ and $\text{In}_{0.5}\text{Ga}_{0.5}\text{As}_{0.5}\text{Sb}_{0.5}$: ab initio Calculations for Pure and Doped Materials. *Chin. Phys. Lett.*, 29 (3), 037302.
- [5] G. Martinez. (1973). Band Inversion in $\text{Pb}_{1-x}\text{Sn}_x\text{Se}$ Alloys under Hydrostatic Pressure. II. Galvanomagnetic Properties, *Phys. Rev.* 45 (8), 4686.
- [6] Zongsong Gan. (2013). Direct laser writing of three-dimensional narrow band gap and high refractive-index PbSe structures in a solution. *Optics Express*, 21 (9), 11202-11208.
- [7] S. Labidi a, M. Labidi. (2011). Modeling of impact toughness of cold formed material by genetic programming. *Computational Materials Science*, 50 (3). 1077–1082.
- [8] A. Miller, G. Saunders and Y. Yogurtcu. (1981). Pressure dependences of the elastic constants of PbTe, SnTe and $\text{Ge}_{0.08}\text{Sn}_{0.92}\text{Te}$. *J. Phys.*, 14 (2), 1569.
- [9] M. Cardona, D and L. Greenaway. (1964). Optical Properties and Band Structure of Group IV-VI and Group V Materials *Phys. Rev.*, 133(5), 1685.
- [10] D. Korn, R. Braunstein. (1972). Reflectivity and Wavelength-Modulation-Derivative Reflectivity of $\text{Pb}\{1-x\}\text{Sn}\{x\}\text{Te}$, *Phys. Rev.*, 24 (5), 4837.
- [11] A. I. Lebedev and I. A. Sluchinskaya. (1994) Ferroelectric phase transitions in IV-VI semiconductors associated with off-center ions. *Ferroelectrics*, 157 (1), 275-280.
- [12] T. Seetawan and H. Wattanasarn, (2012). First Principle Simulation Mechanical Properties of PbS, PbSe, CdTe and PbTe by Molecular Dynamics. *Procedia Engineering*, 32 (1), 609 – 613.
- [13] S. Q. Wang, (2002). Plane-wave pseudopotential study on mechanical and electronic properties for IV and III-V crystalline phases with zinc-blende structure. *Physical Review* 66 (40), 235111..
- [14] S. Kumar, M. A. M. Khan, A. S. Khan and M. Husain. (2004). Studies on Vacuum Evaporated $\text{PbS}_{1-x}\text{Se}_x$ Thin Films, *Optical Materials*, 25 (1) 25-32.
- [15] R. B. Schoolar, J. D. Jensen, G. M. Black, S. Foti and A. C. Bouley. (1980) Multispectral $\text{PbS}_x\text{Se}_{1-x}$ and $\text{Pb}_y\text{Sn}_{1-y}\text{Se}$ Photovoltaic Infrared Detectors,” *Infrared Physics*, 20 (4), 271-275.
- [16] P. Hohenberg and W. Kohn. (1964). Inhomogeneous Electron Gas. *Physical Review B*, 136 (2), B864- B871.
- [17] A. Bouhemadou, M.A. Ghebouli, (2013). Structural, elastic, electronic and lattice dynamical properties of III-P quaternary alloys matched to AIP. 16 (3) 718–726.
- [18] W. Li and J.-F. Chen. (2010). Electronic and Elastic Properties of PbS under Pressure *Physica B: Condensed Matter*, 405. (5) 1279-1282.
- [19] M.C. Payne, M.P. Teter, D.C. Allen, T.A. Arias, J.D. Joannopolous. (1992). Iterative minimization techniques for *ab initio* total-energy calculations: molecular dynamics and conjugate gradients *Rev. Mod. Phys.* 64 1045.
- [20] H.J. Monkhorst, J.D. Pack, (1976). Special points for Brillouin-zone integrations. *Phys. Rev.*, 13(2), 5188.
- [21] M. Oloumi, C.C. Matthai, (1990) Electronic structure and band discontinuities in the InAs/GaAs system. *J. Phys. Condens. Matter*, 43 (2) 5153.

- [22] M. Labidi, H. Meradji, (2011). Structural, electronic, optical and thermodynamic properties of pbs, pbse and their ternary alloy. *Modern Physics Letters B*, 25 (7), 473–486.
- [23] S. Kacimi, A. Zaoui, (2008) Ab initio study of cubic PbS_xSe_{1-x} alloys. *Journal of Alloys and Compounds*, 462 (1), 135–141.
- [24] Mazin S. Othman, (2013). Simulation Mechanical Properties of Lead Sulfur Selenium under Pressure. *Journal of Modern Physics*, 4 (1), 185-190.
- [25] Wenshan Cai, Vladimir Shalaev (2010). *Optical Metamaterials*, Springer Dordrecht Heidelberg London. 978 (1) 4419-1150-6.
- [26] E. A. Davis and N. F. Mott. (1970) Conduction in non-crystalline systems V. Conductivity, optical absorption and photoconductivity in amorphous semiconductors. 22, 179, *Philosophical Magazine*.
- [27] Yuhua Wang, Lingli Wang, (2007). Electronic structure and linear optical properties of $YAl_3(BO_3)_4$. *J. Appl. Phys.*, 102 (2), 013711.
- [28] Charles C. Kim, J. W. Garland, (1992). Modeling the optical dielectric function of semiconductors: Extension of the critical-point parabolic-band approximation. *Phys. Rev. B*, 45 (1), 11749–11767
- [29] Z. Yin and F. W. Smith, (1990). Optical dielectric function and infrared absorption of hydrogenated amorphous silicon nitride films: Experimental results and effective-medium-approximation analysis. *Phys. Rev. B*, 42 (2), 3666–3675